JOURNAL OF SPACECRAFT AND ROCKETS
Vol. 29, No. 6, November–December 1992

Parametric Study of Manned Aerocapture Part II: Mars Entry

J. E. Lyne*
Eloret Institute, Palo Alto, California 94303
A. Anagnost†
Stanford University, Stanford, California 94305
and
M. E. Tauber‡
NASA Ames Research Center, Moffett Field, California 94035

A parametric study of aerocapture for manned Mars missions has been conducted. The variation of entry corridor width and stagnation-point heating with vehicle entry velocity, ballistic coefficient, and lift-to-drag ratio were examined. To maximize corridor widths, the aerocapture maneuvers employed variable bank-angle trajectories. Vehicles with an L/D of 0.4–0.5 were found to provide an entry corridor width of at least 1 deg for approach velocities up to 10 km/s. Vehicle convective heating calculations were performed assuming a fully catalytic "cold" wall; radiative heating was computed assuming that the shock layer was in thermochemical equilibrium. It was found that for entry velocities below approximately 7 km/s, radiative cooling may be possible for the thermal protection system. At higher entry speeds, ablative heat shields must be used. Maximum integrated stagnation-point heat loads were found to be equivalent to or less than those experienced by the Space Shuttle on a typical re-entry.

Nomenclature

A	= vehicle reference area for aerodynamic coefficients, m^2
C_D	= drag coefficient
D	= drag, N
L	= lift, N
m	= vehicle mass, kg
m/C_DA	= ballistic coefficient, kg/m^2
V_e	= vehicle velocity on entering the Martian atmosphere, km/s

Introduction

DURING the last 30 years, several investigators have shown that the use of aerobraking at Mars on a manned mission could result in a substantial decrease in the initial weight required in low Earth orbit.[1,2] For such a mission to be successful, the vehicle must dissipate enough energy in its initial pass through the atmosphere to be captured into a planetocentric orbit without overheating or subjecting the crew and structure to excessive deceleration. The location and width of the entry corridor depend on the vehicle's arrival velocity, V_e, and aerodynamic characteristics (ballistic coefficient m/C_DA and lift-to-drag ratio L/D).

Various mission architectures differ markedly with respect to the arrival conditions at Mars.[3–5] Launch date and the type of interplanetary trajectory flown significantly influence the atmospheric entry velocity; as a result, recent studies reveal a range of probable entry speeds from 6 to 10 km/s (see Fig. 1).[6] Mission plans also differ with respect to the aerobrake designs. Both blunt, low L/D configurations[6] similar to the Aeroassist Flight Experiment vehicle and relatively high lift, winged vehicles[4,7] (L/D over 1.0) have been proposed.

Because of its impact on required guidance system accuracy, entry corridor width is an important factor in judging a given mission's feasibility. For example, a very narrow entry corridor could result in severe guidance demands requiring an infrastructure of navigational aids in the vicinity of Mars.[8] In addition, peak and integrated heating rates influence mission feasibility via their impact on the weight and nature of the thermal protection system (TPS).[7]

Therefore, this paper presents the results of a parametric study of corridor width and stagnation-point heating for a range of probable mission designs and vehicle configurations. Entry velocities are varied from 6 to 10 km/s, L/Ds from 0.1 to 1.0, and ballistic coefficients from 100 to 500 kg/m^2.

Trajectories

Trajectory Constraints

For an aerocapture maneuver to be successful, the atmospheric trajectory must satisfy several constraints. First, the

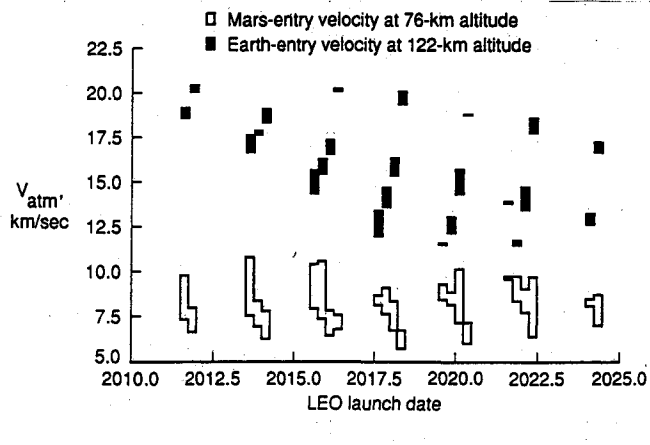

Fig. 1 Entry velocity vs launch date.

Received July 2, 1991; presented as Paper 91-2871 at the AIAA Atmospheric Flight Mechanics Conference, New Orleans, LA, Aug. 12–14, 1991; revision received April 13, 1992; accepted for publication April 24, 1992.

*Research Scientist, Thermosciences Division, NASA Ames Research Center. Student Member AIAA.

†Graduate Student, Department of Aeronautics and Astronautics. Student Member AIAA.

‡Senior Research Scientist, Thermosciences Division, Mail Stop 229-3. Associate Fellow AIAA.

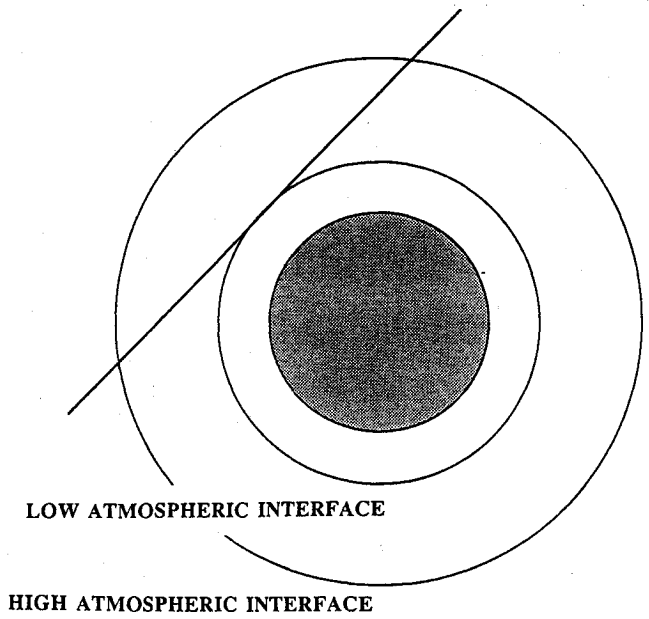

Fig. 2 Effect of entry altitude on entry angle.

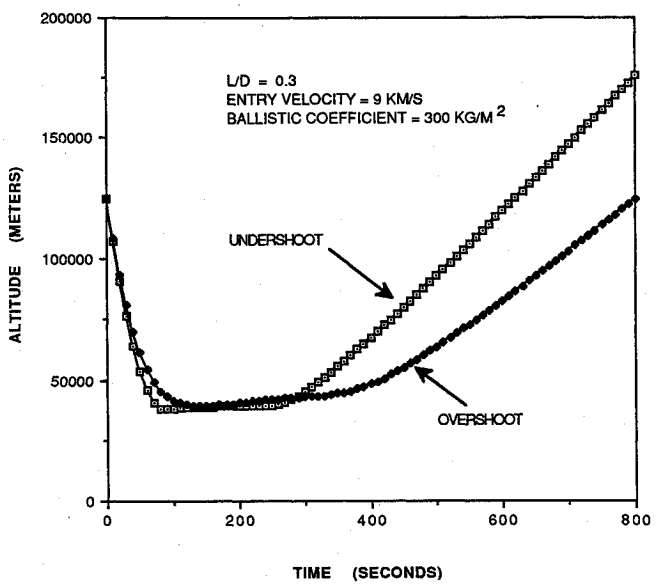

Fig. 3 Typical aerocapture trajectories.

vehicle must dissipate the proper amount of energy to transition from a hyperbolic approach trajectory into the target orbit. (A small thrust maneuver will be required at apoapsis to lift the periapsis to the desired altitude.) For this study, the vehicle was placed in a low Mars orbit with a period of approximately 1.8 h. This period was selected because it affords a relatively benign descent to the surface and results in a somewhat wider entry corridor for low L/D vehicles entering at 6 to 7 km/s.[9] However, it should be noted that there are valid arguments for choosing other parking orbits. For example, longer period, higher energy orbits will result in lower propulsion requirements for trans-Earth injection.[8,10]

The entry trajectory's primary constraint was the deceleration tolerance of a crew that has been physiologically decondi-

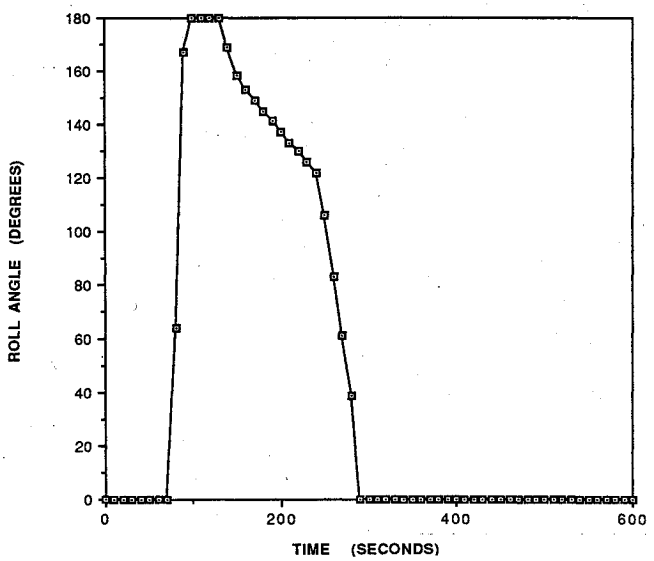

Fig. 4 Vehicle roll angle history.

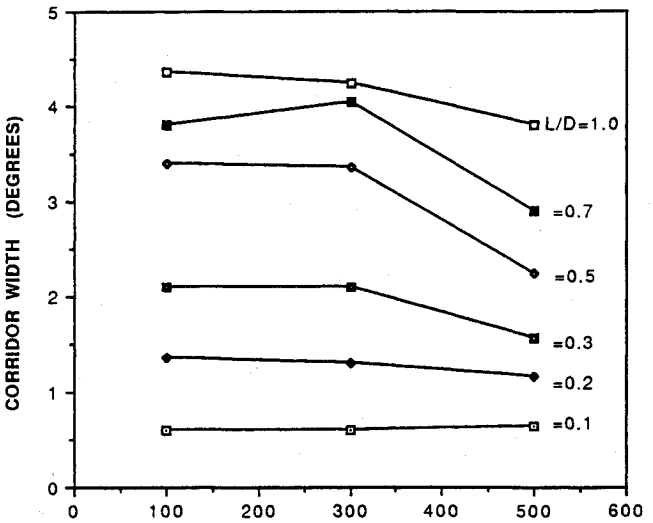

a) Entry velocity = 6000 m/s

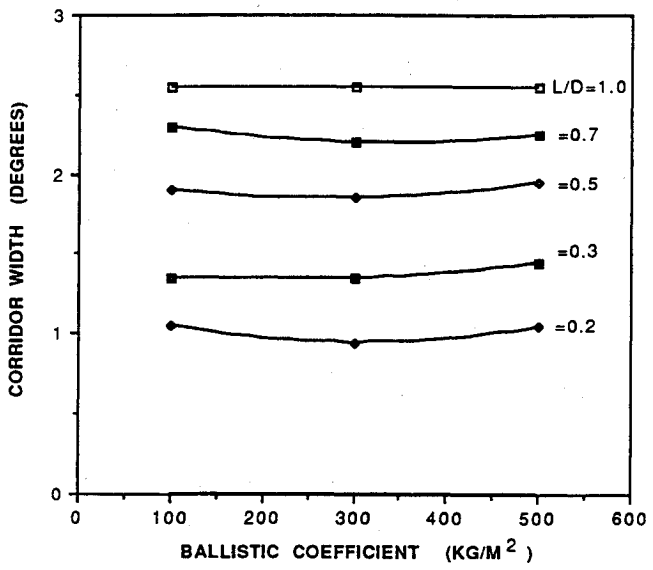

b) Entry velocity = 8000 m/s

Fig. 5 Corridor width vs ballistic coefficient.

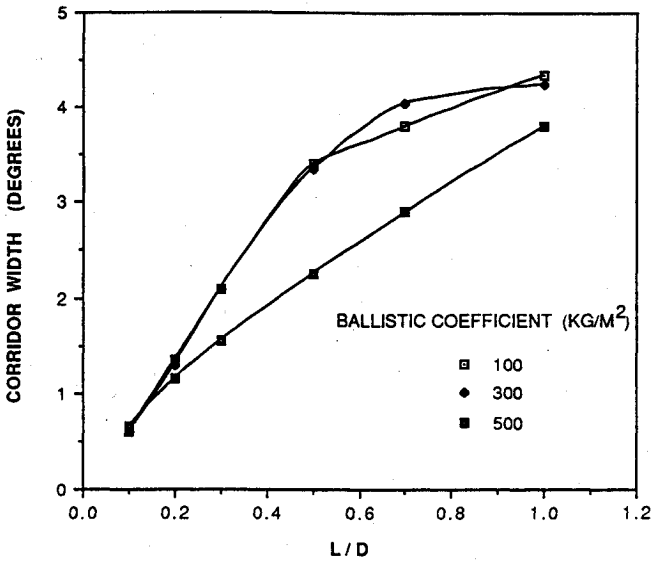

a) Entry velocity = 6000 m/s

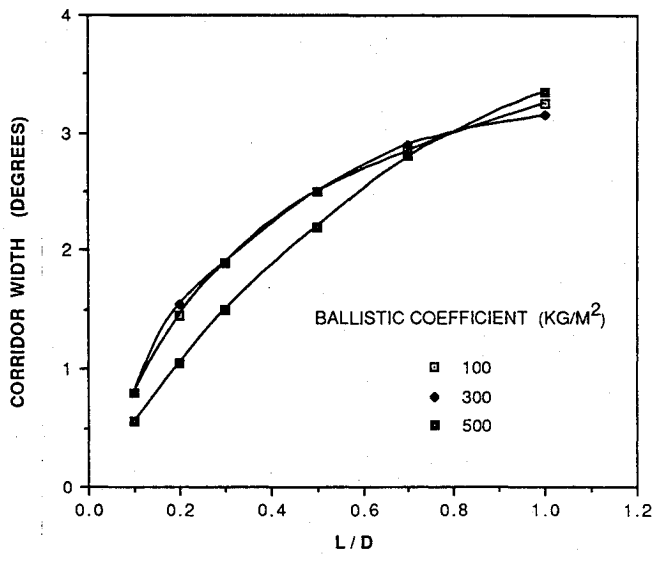

b) Entry velocity = 7000 m/s

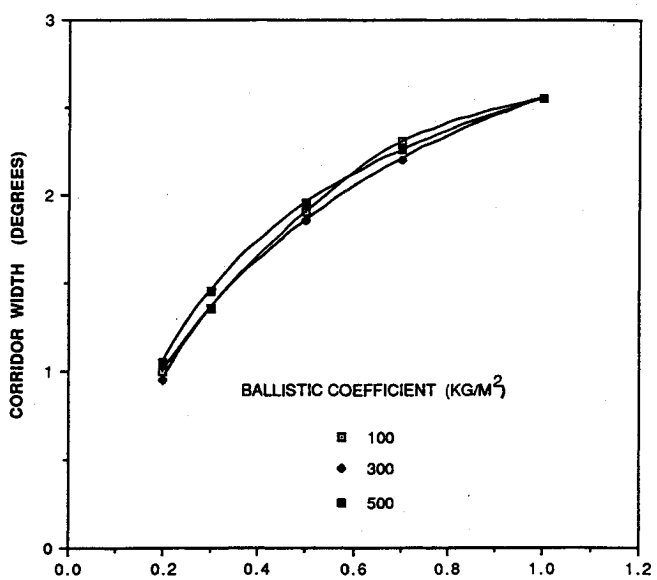

c) Entry velocity = 8000 m/s

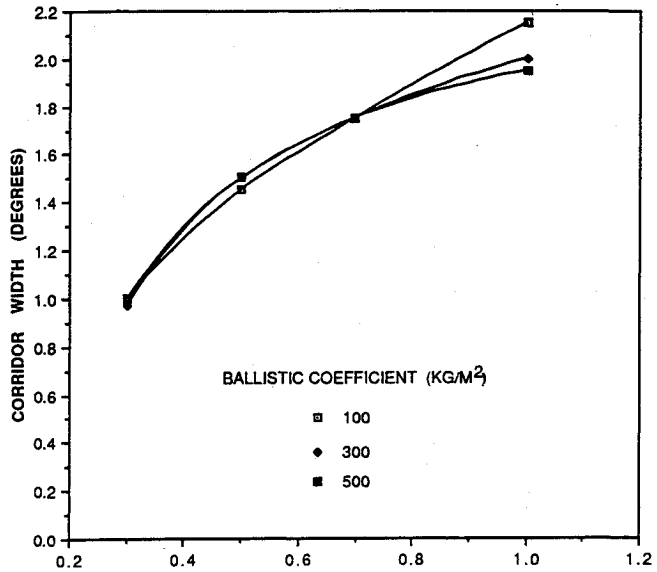

d) Entry velocity = 9000 m/s

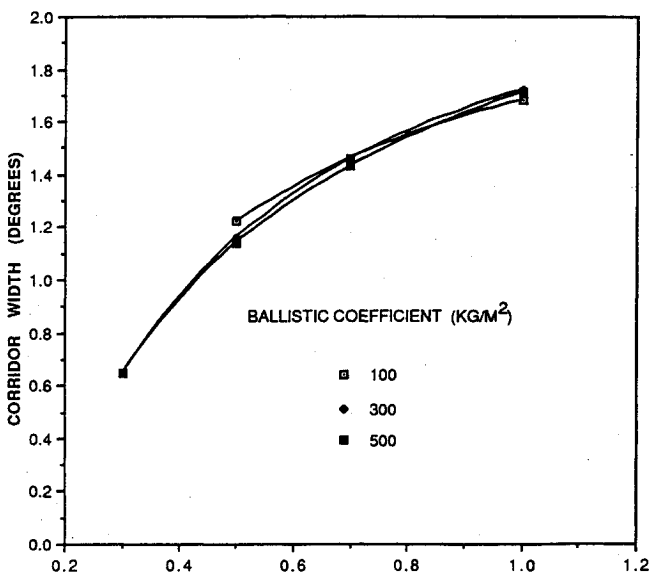

e) Entry velocity = 10,000 m/s

Fig. 6 Corridor width vs *L/D*.

tioned by several months of weightlessness. A 5-*g* (Earth) peak deceleration limit was chosen for use in this study, consistent with the rationale in Part I.

An additional constraint on the trajectory prevented the aerobrake from passing below an altitude of 30 km at any point; this was designed to prevent collisions with mountains which may rise as much as 25 km above the mean surface.

Atmospheric Model

The Martian atmospheric model was based on Viking lander data.[11] The density was fitted with a series of three exponential expressions, and the entry interface was assumed to be at 125 km. The atmosphere was assumed to be insensible at higher altitudes. This altitude has been used as the atmospheric interface in previous guidance and control studies.[12] The atmosphere was assumed to be nonrotating and was not varied with latitude, longitude, or season.

Table 1 Variation of nose radius with L/D

L/D	Nose radius, m
0.3	16.0
0.5	11.7
1.0	1.00

It should be noted that the entry angle depends on the altitude at which entry is measured. Although this is a purely geometric effect (see Fig. 2), it must be considered when comparing the results of different studies. Using the empirical results provided in Part I, the vehicles' peak L/D was decreased at high altitudes to account for increased laminar skin friction relative to wave drag in the high-altitude flight regime.

Trajectory Calculations

The trajectory of a vehicle in unpowered flight through a nonrotating atmosphere is described by a system of three first-order, ordinary differential equations.[13] For this study, these equations were solved by two algorithms very similar to those described in Part I. These computer programs automatically found the overshoot and undershoot trajectories for a given set of entry conditions. A variable bank angle scheme was used to maximize corridor width. A more detailed description of the algorithms is provided in Ref. 14.

Heating Calculations

Stagnation-point heating rate and integrated heat load were calculated as described in Refs. 4 and 15. Both convective and equilibrium radiative processes were considered. For the cases that will be discussed here, the wall was assumed to be fully catalytic and "cold" (nonablating and, therefore, not affecting the heat transfer via alterations of the boundary layer). All calculations were made assuming that the inviscid shock layer is in equilibrium.

Since the study involved vehicles with a wide range of L/D, the nose radii used for heating calculations had to be varied. The high L/D vehicles intrinsically have much smaller nose radii than low L/D configurations as indicated by the values shown in Table 1.

Results

Corridor Width

Figure 3 shows typical entry trajectories for overshoot and undershoot cases; the corresponding deceleration pulses are comparable with that for the Soyuz entry capsule described in Part I. The vehicle bank-angle history used to achieve the undershoot trajectory for this particular Mars aerocapture is illustrated in Fig. 4.

Entry corridor width was found to be relatively insensitive to ballistic coefficient, especially at moderate and high entry velocities (Fig. 5). However, L/D was shown to profoundly influence the corridor width for all potential entry speeds, as is depicted in Fig. 6. The variation of corridor width with entry velocity is illustrated in Fig. 7 for ballistic coefficients of 100, 300, and 500 kg/m^2. The curves for low L/D vehicles are qualitatively different from those for the higher L/D configurations; this resulted because different factors determined the undershoot boundaries. In most cases, the steepest entry angle was constrained by the 5-g limit. However, for scenarios with low entry velocities and low L/D, the undershoot boundary was determined by the requirement that the vehicle have enough energy to skip into the desired orbit. For steeper entries, too much energy was dissipated, and the target orbit was not attainable. These cases lie to the left of the dashed line in Fig. 7. As can be seen, this effect becomes more pronounced as the ballistic coefficient increases. Under such circumstances, the undershoot trajectory may never approach the 5-g limit. In this situation, a low-altitude, low-energy

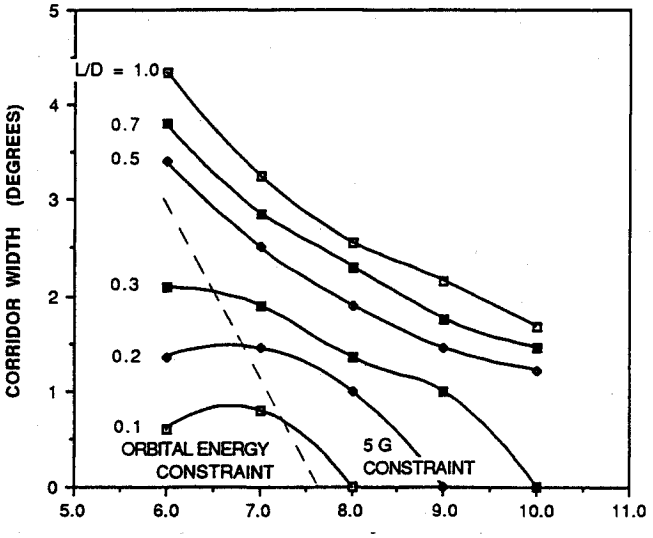

a) Ballistic coefficient = 100 kg/m^2

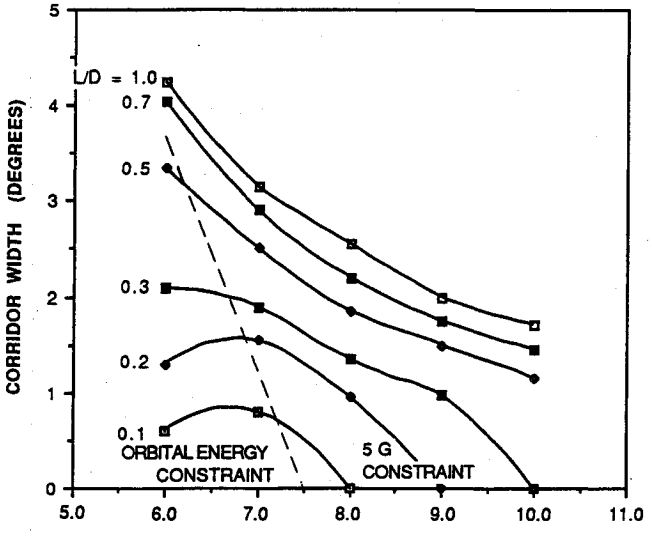

b) Ballistic coefficient = 300 kg/m^2

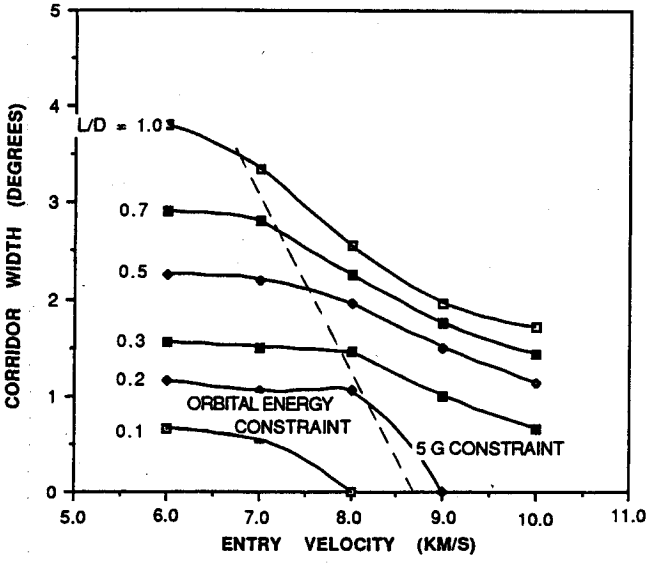

c) Ballistic coefficient = 500 kg/m^2

Fig. 7 Corridor width vs entry velocity.

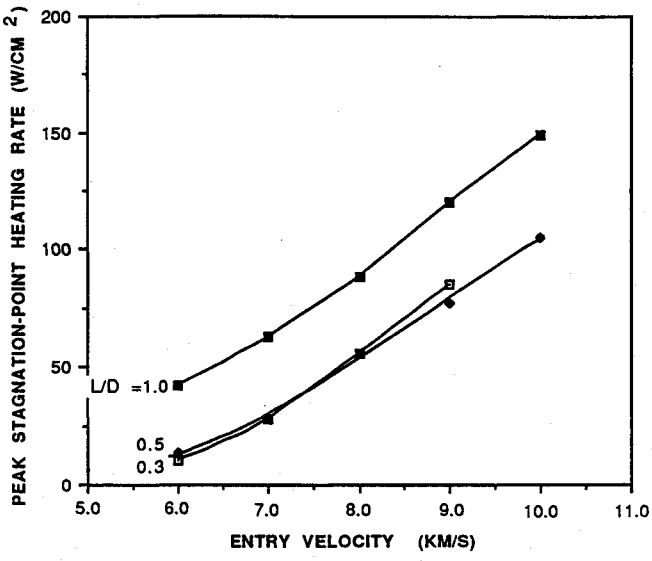

a) Ballistic coefficient = 100 kg/m^2

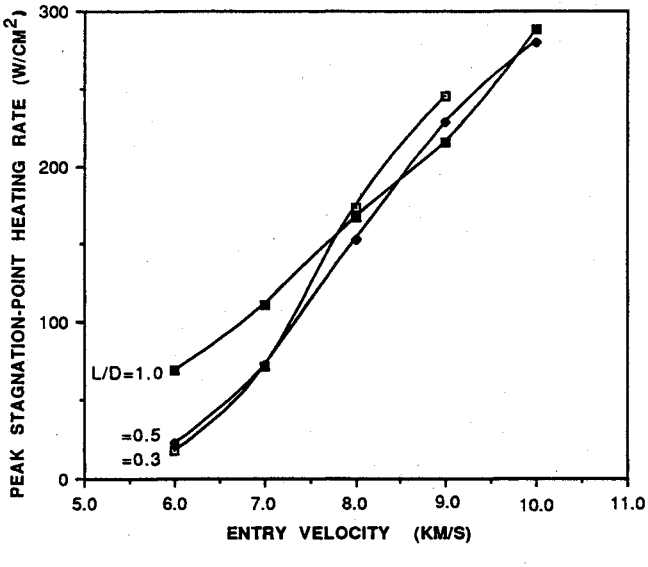

b) Ballistic coefficient = 300 kg/m^2

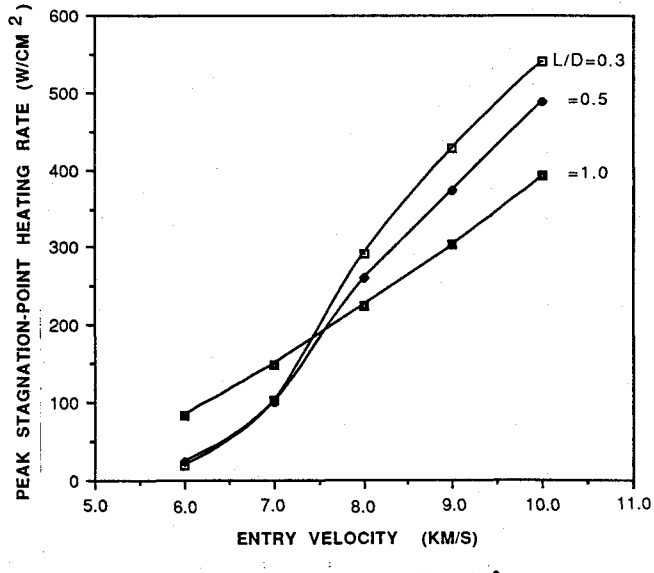

c) Ballistic coefficient = 500 kg/m^2

Fig. 8 Undershoot trajectory peak stagnation-point heating.

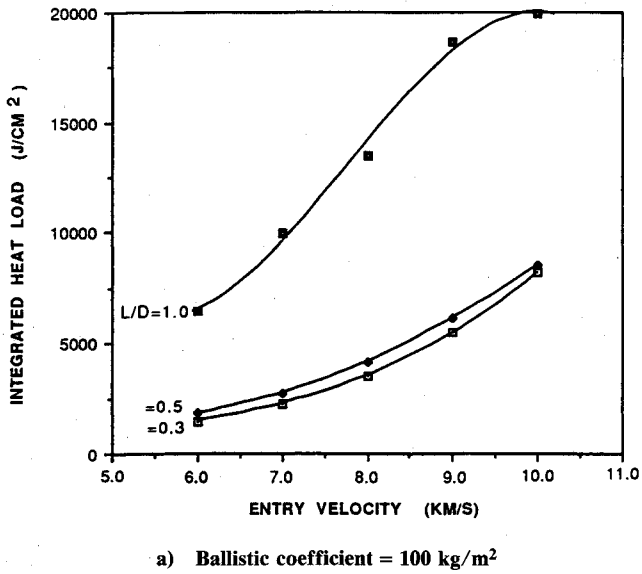

a) Ballistic coefficient = 100 kg/m^2

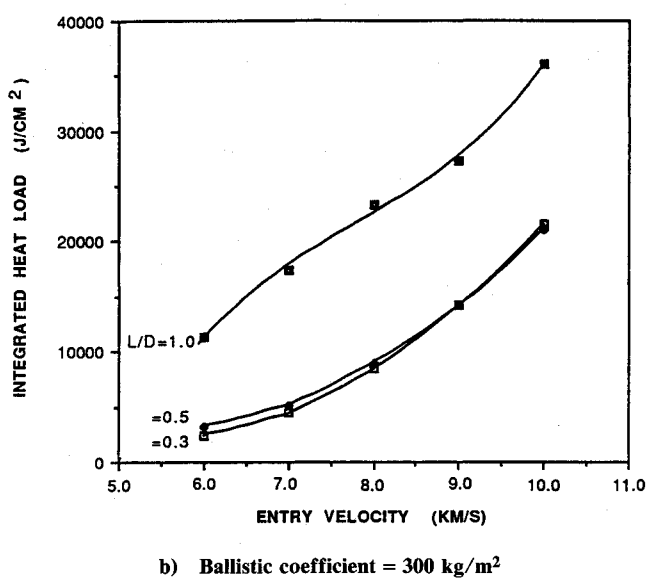

b) Ballistic coefficient = 300 kg/m^2

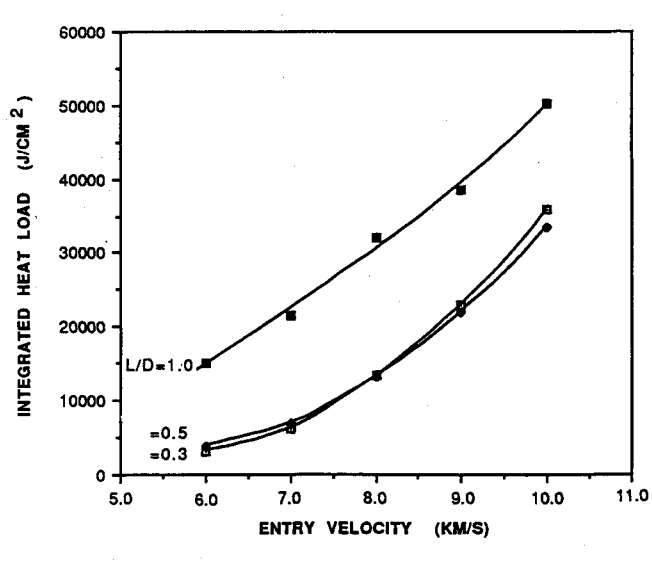

c) Ballistic coefficient = 500 kg/m^2

Fig. 9 Overshoot trajectory integrated heat load.

target orbit provides a steeper undershoot boundary and a wider entry corridor.

The required corridor width will depend on the accuracy of the encounter navigation system and the degree of knowledge of the Martian atmosphere. Recent studies have examined navigation errors from 0.05 to 1.5 deg[8,12]; aerodynamic and atmospheric dispersions must be considered in addition to these navigational errors. Although uncertainties regarding future technology make it difficult to predict the required corridor width precisely, several authors have adopted a 1-deg limit.[6,7] If this criterion is used here, the aerobrake is found to require a minimum L/D of 0.3 for entries up to 9 km/s or 0.4 to 0.5 for entries up to 10 km/s.

Heating Rates

Stagnation-point peak heat transfer rate, which is greatest for the undershoot trajectories, is shown in Fig. 8 as a function of entry velocity. Maximum heating rate determines the type of material required for the thermal protection system. For a single-use vehicle, radiatively cooled surfaces can tolerate rates as calculated here up to approximately 100 W/cm^2 since the present results are for a fully catalytic surface; the use of a noncatalytic surface such as ceramic tiles should reduce the heating rates significantly.[4] On the Space Shuttle, the peak heating experienced by the radiatively cooled tiles is about half of this value since Shuttle tiles must endure multiple entries. If peak heating exceeds 100 W/cm^2, low-density ablative materials must be employed. It is evident from Fig. 8 that for certain mission scenarios, a radiatively cooled TPS may be practical. However, as ballistic coefficient increases, the vehicle must enter more slowly to remain below the 100 W/cm^2 level. For an m/C_DA of 300 and 500, the peak heating curve for an L/D of 1.0 crosses the other two curves; this result is due to the increasing importance of radiative heating for blunt, low L/D vehicles at high entry velocities. Radiative heating assumes a greater significance for low L/D vehicles than for high L/D configurations since blunt shapes have larger nose radii resulting in thicker shock layers. This effect becomes more pronounced with higher ballistic coefficient and deeper penetration into the atmosphere where the relative importance of radiation is greater.

Integrated Heat Load

Stagnation-point integrated heat load, which is greatest for overshoot trajectories, is shown in Fig. 9 as a function of entry velocity. Vehicles with an L/D of 1.0 experienced a much higher heat load than lower L/D configurations for all velocities and ballistic coefficients. This is caused by the high L/D allowing shallow overshoot boundaries which result in prolonged heating pulses. As entry velocity increases and peak heating rates of blunt, low L/D vehicles become greater than those of high L/D configurations (because of radiation), this disparity becomes less pronounced. For example, in Fig. 9 the heat load for an L/D of 1.0 is approximately four times that for an L/D of 0.5 at an entry speed of 6 km/s; at 9 km/s it is only twice as great. In all but the most extreme case, the integrated heat load is less than the 40 kJ/cm^2 which the Space Shuttle's stagnation point typically experiences.

Conclusions

A parametric study of manned Mars aerocapture was made. The entry vehicle was captured into a low Mars orbit and was required to observe a peak deceleration limit of 5 g. The aerocapture maneuvers employed roll modulation to maximize entry corridor widths. If a 1-deg corridor requirement is assumed, vehicles with an L/D of 0.4–0.5 are found to be satisfactory for entry velocities up to 10 km/s.

Vehicle stagnation-point heating calculations were done assuming a fully catalytic "cold" wall and an inviscid shock layer in thermochemical equilibrium. It was found that for entry velocities below approximately 7 km/s, a thermal protection system consisting of radiatively cooled ceramic tiles may be possible. At higher entry speeds, ablative heat shields must be used. Maximum integrated stagnation-point heat loads were found to be substantially higher for vehicles with an L/D of 1.0 than for blunt, low L/D configurations. However, in all but the most severe case, the total stagnation point heat load was less than that for the Space Shuttle on a typical re-entry.

Acknowledgment

This research is supported by NASA Grant NAGW-1331 to the Mars Mission Research Center.

References

[1]Tauber, M. E. and Seiff, A., "Optimization of Heating of Conical Bodies Making Lifting Hyperbolic Entries into the Atmospheres of Earth and Mars," *Proceedings of the AIAA Entry Technology Conference* (Williamsburg, VA), AIAA, New York, Oct. 1964.

[2]Clark, B., "Manned Mars Missions for the Year 2000," AIAA Paper 89-0512, Jan. 1989.

[3]Walberg, G. D., "A Review of Aerobraking for Mars Missions," International Astronautical Federation, Paper 88-196, Bangalore, India, Oct. 1988.

[4]Tauber, M. E., Bowles, J. V., and Yang, L., "The Use of Aerobraking During Mars Missions," *Journal of Spacecraft and Rockets,* Vol. 27, No. 5, 1990, pp. 514–521.

[5]Braun, R. D., "The Influence of Interplanetary Trajectory Options on a Chemically Propelled Manned Mars Vehicle," *Journal of the Astronautical Sciences,* Vol. 38, No. 3, July–Sept. 1990, pp. 289–310.

[6]Braun, R. D., Powell, R. W., and Hartung, L. C., "The Effect of Interplanetary Trajectory Options on a Manned Mars Aerobrake Configuration," NASA TP-3019, July 1990.

[7]Tauber, M., Chargin, M., Henline, W., Chiu, A., Yang, L., Hamm, K. R., Jr., and Minra, H., "Aerobrake Design Studies for Manned Mars Missions," AIAA Paper 91-1344, June 1991.

[8]Wilcockson, W. H., "L/D Requirements for Mars Aerocapture Missions," AIAA Paper 90-2937, Aug. 1990.

[9]Gamble, J. D., "JSC Pre-Phase A Study: Mars Rover Sample Return Mission Aerocapture, Entry, and Landing Element," NASA Rept. JSC-23230, May 1989.

[10]Babb, G. R., and Stump, W. R., "Mars Orbit Selection," NASA TM 89320, June 1986.

[11] Seiff, A., and Kirk, D. B., "Structure of the Atmosphere of Mars in Summer at Mid-Latitudes," *Journal of Geophysical Research,* Vol. 82, No. 28, Sept. 1977, pp. 4364–4378.

[12]Brand, T. J., Fuhry, D. P., and Shepperd, S. W., "An Onboard Navigation System Which Fulfills Mars Aerocapture Guidance Requirements," AIAA Paper 89-0629, Jan. 1989.

[13]Vinh, N. X., Busemann, A., and Culp, R., *Hypersonic and Planetary Flight Mechanics,* Univ. of Michigan Press, Ann Arbor, MI, 1980, pp. 100–107.

[14]Lyne, J. E., "Physiologically Constrained Aerocapture for Manned Mars Missions," Doctoral Dissertation, North Carolina State Univ., Raleigh, NC, 1992.

[15]Tauber, M. E., and Sutton, K., "Stagnation Point Radiative Heating Relations for Earth and Mars Entries," *Journal of Spacecraft and Rockets,* Vol. 28, No. 1, 1991, pp. 40–42.

Gerald T. Chrusciel
Associate Editor